Turkish Journal of Medical Sciences

Volume 53 | Number 6 Article 34

2023

Microstructural evaluation of the brain with advanced magnetic resonance imaging techniques in cases of electrical status epilepticus during sleep (ESES)

HANİFE GÜLDEN DÜZKALIR

BARIŞ GENÇ

SAFİYE GÜNEŞ SAĞER

AYBERK TÜRKYILMAZ

HEDİYE PINAR GÜNBEY

Follow this and additional works at: https://journals.tubitak.gov.tr/medical

 Part of the Medical Sciences Commons

Recommended Citation

DÜZKALIR, HANİFE GÜLDEN; GENÇ, BARIŞ; SAĞER, SAFİYE GÜNEŞ; TÜRKYILMAZ, AYBERK; and GÜNBEY, HEDİYE PINAR (2023) "Microstructural evaluation of the brain with advanced magnetic resonance imaging techniques in cases of electrical status epilepticus during sleep (ESES)," *Turkish Journal of Medical Sciences*: Vol. 53: No. 6, Article 34. https://doi.org/10.55730/1300-0144.5754
Available at: https://journals.tubitak.gov.tr/medical/vol53/iss6/34

This Article is brought to you for free and open access by TÜBİTAK Academic Journals. It has been accepted for inclusion in Turkish Journal of Medical Sciences by an authorized editor of TÜBİTAK Academic Journals. For more information, please contact academic.publications@tubitak.gov.tr.

TÜBİTAK

Turkish Journal of Medical Sciences

http://journals.tubitak.gov.tr/medical/

Research Article

Turk J Med Sci
(2023) 53: 1840-1851
© TÜBİTAK
doi:10.55730/1300-0144.5754

Microstructural evaluation of the brain with advanced magnetic resonance imaging techniques in cases of electrical status epilepticus during sleep (ESES)

Hanife Gülden DÜZKALIR[1,*], Barış GENÇ[2], Safiye Güneş SAĞER[3], Ayberk TÜRKYILMAZ[4], Hediye Pınar GÜNBEY[1]

[1]Department of Radiology, Kartal Dr. Lütfi Kırdar City Hospital, İstanbul, Turkiye
[2]Department of Radiology, Samsun Education and Research Hospital, Samsun, Turkiye
[3]Department of Pediatric Neurology, Kartal Dr. Lütfi Kırdar City Hospital, İstanbul, Turkiye
[4]Department of Medical Genetics, Faculty of Medicine, Karadeniz Technical University, Trabzon, Turkiye

Received: 01.08.2023 • **Accepted/Published Online:** 25.10.2023 • **Final Version:** 12.12.2023

Background/aim: The cause and treatment of electrical status epilepticus during sleep (ESES), one of the epileptic encephalopathies of childhood, is unclear. The aim of this study was to evaluate possible microstructural abnormalities in the brain using advanced magnetic resonance imaging (MRI) techniques in ESES patients with and without genetic mutations.

Materials and methods: This research comprised 12 ESES patients without structural thalamic lesions (6 with genetic abnormalities and 6 without) and 12 healthy children. Whole-exome sequencing was used for the genetic mutation analysis. Brain MRI data were evaluated using tractus-based spatial statistics, voxel-based morphometry, a local gyrification index, subcortical shape analysis, FreeSurfer volume, and cortical thickness. The data of the groups were compared.

Results: The mean age in the control group was 9.05 ± 1.85 years, whereas that in the ESES group was 9.45 ± 2.72 years. Compared to the control group, the ESES patients showed higher mean thalamus diffusivity ($p < 0.05$). ESES patients with genetic mutations had lower axial diffusivity in the superior longitudinal fasciculus and gray matter volume in the entorhinal region, accumbens area, caudate, putamen, cerebral white matter, and outer cerebellar areas. The superior and middle temporal cortical thickness increased in the ESES patients.

Conclusion: This study is important in terms of presenting the microstructural evaluation of the brain in ESES patients with advanced MRI analysis methods as well as comparing patients with and without genetic mutations. These findings may be associated with corticostriatal transmission, ictogenesis, epileptogenesis, neuropsychiatric symptoms, cognitive impairment, and cerebellar involvement in ESES. Expanded case-group studies may help to understand the physiology of the corticothalamic circuitry in its etiopathogenesis and develop secondary therapeutic targets for ESES.

Key words: Electrical status epilepticus during sleep, microstructural analysis, morphometry, genetic mutation, tractus-based spatial statistics

1. Introduction

Electrical status epilepticus during sleep (ESES) is a type of epileptic encephalopathy that develops in childhood, worsens in middle and late childhood, and may heal spontaneously before puberty [1]. Cognitive impairment, electrical status epilepticus during sleep , and epileptiform activity without rapid eye movements are characteristic findings. The disease spectrum includes frontal lobe executive dysfunctions, behavioral abnormalities, learning problems, and intellectual deficiencies. Early detection and treatment are critical to prevent serious mental problems and resistant epilepsies [2,3].

Cranial magnetic resonance imaging (MRI) is the recommended imaging modality for ESES diagnosis. In the literature, ESES studies have mainly focused on the thalamus. Experimental studies have linked the amplification of oscillatory discharges in the cortico-thalamo-cortical (CTC) network to lesions in the reticular nucleus of the thalamus [3]. Thalamic volume loss, early developmental lesions, and functional impairment have been linked to CTC network disruption [4]. Although thalamic lesions have been linked to ESES [3], the cause of ESES without structural abnormalities is still not clearly understood.

Conventional MRI can detect macrostructural abnormalities such as thalamic damage in ESES, but microstructural changes in grey and white matter (WM)

* Correspondence: hanifeduzkalir@gmail.com.tr

This work is licensed under a Creative Commons Attribution 4.0 International License.

are difficult to detect with conventional sequences. One of the advanced MRI methods, diffusion tensor imaging (DTI), objectively measures water transport to characterize WM microstructure in vivo noninvasively. The main DTI parameters are fractional anisotropy (FA), which gives a summary measure of microstructural integrity; mean diffusion (MD), which describes overall diffusion and gives a measure of average diffusion in 3 directions; radial diffusion (RD); and axial diffusion (AD), which provides more explicit and specific information about the microstructure. Tractus-based spatial statistics (TBSS) is an automated, voxel-based statistical analytical DTI method developed to objectively compare diffusion properties between subjects independently of the observer [5]. Voxel-based morphometry (VBM) compares groups using a probability map based on the likelihood of gray matter (GM), WM, or cerebrospinal fluid (CSF) in voxels [6]. The local gyrification index measures the amount of folding, detects folding differences, and may indicate developmental disorders [7]. Subcortical shape analysis can precisely detect shape changes before volume changes [8].

The aim of this study was to evaluate possible microstructural abnormalities in the brain in ESES patients with and without genetic mutations using DTI TBSS, VBM, the local gyrification index, subcortical shape analysis, FreeSurfer volume, and cortical thickness analysis methods in cranial MRI.

2. Materials and methods

2.1. Study design

This observational cross-sectional study was performed at a single center. The study was performed in adherence with the Declaration of Helsinki,. The study was authorized by the ethics committee of our hospital. Written informed consent was given by the parents.

2.2. Patients and control groups

ESES patients (n = 20) aged 5–17 years were included in the study. The inclusion criteria were:

- A diagnosis of ESES by a pediatric neurologist based on the International League Against Epilepsy categorization, electrical status epilepticus during slow wave sleep and generalized bilateral symmetrical spike and slow wave discharges on electroencephalogram.
- The exclusion of other epileptic syndrome diagnoses.
- The absence of any other underlying etiological pathology (corpus callosum disruption or lesion, localized cortical lesion, hippocampal atrophy, cerebral or cerebellar atrophy, polymicrogyria or heterotopia, arachnoid cyst, hydrocephalus, perinatal ischemia, or thalamic lesion).

Of the patients, 4 were excluded due to thalamic asymmetry, 2 due to structural abnormalities, and 2 due to prenatal ischemia sequelae. Thus, 12 ESES patients were included.

The control group consisted of age- and sex-matched healthy patients who were referred to our radiology clinic for MRI scanning and had no abnormal findings on brain MRI, no clinical or laboratory data that could affect their neurological status, and no known diseases. Patients with MRI artifacts and incidental benign abnormalities such as arachnoid cysts and giant cisterna magna were excluded from the control group.

2.3. Molecular study

For the molecular study, 2 mL of peripheral blood was drawn from each ESES patient and into EDTA tubes. The QIAamp DNA Blood Mini QIAcube Kit (Qiagen, Hilden, Germany) was used to isolate genomic DNA from peripheral blood leucocytes according to the manufacturer's instructions. All of the coding regions of the patients' human genomes were sequenced using the QIAseq Human Exome Kit according to the manufacturer's instructions (Qiagen). Paired-end sequencing (150 bp) was performed using a NovaSeq 6000 device (Illumina Inc., San Diego, CA, USA) according to the manufacturer's instructions. The guardians of the patients were informed about the study in person, face-to-face, and written informed consent for the genetic analysis was obtained.

2.4. MRI technique and analysis methods

Imaging was performed with a 1.5 Tesla (T) MRI scanner (Philips Ingenia, Netherlands). Axial spin echo T1-weighted (repetition time/echo time (TR/TE) = 470–570/12–30 ms), axial and sagittal T2-weighted (TR/TE = 4500–6000/90–110 ms), axial and coronal fluid-attenuated inversion recovery (TR/TE = 6000–9000/100–120 ms), diffusion weighted imaging (DWI) (b = 0, 500, 1000), axial diffusion tensor imaging (DTI) (single-shot spin echo-planar imaging and acceleration factor 2 (TR/TE = 7721/96 ms, slice thickness = 2 mm, field of view (FOV) = 230, matrix = 128 × 128, number of excitations = 2, 2 mm, isotropic resolution, interslice gap = 0 mm, number of gradient directions = 16, b values = 0 and 1000 s/mm^2), high-resolution 3D-T1W (TR/TE = 7. 2/33 ms, matrix = 256 × 256 pixels, number of signals averaged = 1, FOV = 256 mm, slice thickness = 1 mm; gap = 0 mm; flip angle = 8°) sequences were used to obtain structural images of the whole brain for anatomical reference. All of the sequences, except those 3D-T1W, were acquired with a slice thickness of 5 mm.

The images were evaluated by a radiologist experienced in neuroradiology. The ESES patients with and without genetic mutations and the control group were compared.

2.4.1. DTI and TBSS analysis

The DTI and TBSS analysis began with DTI eddy current artifact adjustments on the cranial MR images. Then, FA,

AD, MD, and RD maps were obtained with DTIFit. The Forensic Science Laboratory (FSL)-Oxford Centre for Functional Magnetic Resonance Imaging of the Brain's (FMRIB) Integrated Registration and Segmentation Tool (FIRST), a model-based registration and segmentation program, automatically segmented the 3-dimensional (3D)-T1W thalamus images. The FMRIB Linear Image Registration Tool (FLIRT) program aligned the T1W and DTI images. The mean FA, MD, RD, and AD values of the segmented thalamus mask volumes of the aligned images were automatically calculated (Figure 1). The TBSS technique, which is part of the FSL software, was used for the DTI analysis of the WM tract microstructural changes (Figure 2). The Mann–Whitney U test was used to compare the thalamus FA, MD, RD, and AD values of the groups.

2.4.2. VBM-local gyrification index analysis

The 3D T1W images were analyzed using the computational anatomy toolbox (CAT12) (http://dbm.neuro.uni-jena.de/cat/) program implemented in SPM12 (https://www.fil.ion.ucl.ac.uk/spm) running in MATLAB (version 2013a, MathWorks, Natick, MA, USA). The hemispheric surface was reconstructed via projection-based thickness (PBT) automatic reconstruction [9]. The GM, WM, and CSF were analyzed using the original T1W images. The GM images were normalized to an Institute of Neurology (MNI) template. The CAT12 was homogeneity-checked [6]. The GM, WM, and CSF volumes were summed. The GM volume was compared across groups, and voxel density analysis was performed. The indentation index is the ratio of absolute mean curvature of the outer brain surface to the outer surface excluding sulci [10]. Using a standard thalamic mask, the whole brain and 2 regions of interest (ROIs) were compared. All of the ROIs were analyzed simultaneously for the left and right hemispheres, and the automatic anatomical labeling (AAL) atlas revealed the affected brain regions [6].

2.4.3. Subcortical shape analysis

This method used FSL-FIRST to segment the T1W images. The deformable surfaces of the deep GM structures automatically parameterized the volumetric labels. Multivariate Gaussian assumptions collected and modeled the normalized surface intensities. Next, the shape was averaged using the main components. After automated segmentation, all of the subcortical structures were carefully confirmed. Multivariate testing in the 3D vertex coordinates was performed in the vertex-wise shape analysis. The false discovery rate (FDR) or surface-based cluster corrections were evaluated for each vertex separately. The coordinates of each vertex were transferred back and studied in standard space or another space. Alignment eliminated the global rotation and translation between the subjects. For each vertex, the multivariate general linear model (MVGLM) with Pillai's Trace provided a multivariate F-test sensitive to coordinate changes. The variables were age, sex, and total brain volume. The thalamus, hippocampus volumes, amygdala, caudate, and putamen were extracted. Statistical significance was accepted as $p < 0.05$ (FDR-corrected) [11]. IBM SPSS Statistics for Windows 22.0 (IBM Corp., Armonk, NY, USA) was used for the statistical comparison.

2.4.4. FreeSurfer volume and cortical thickness analysis

For accuracy, surface-based cortical thickness analysis models were made of the whole surface. FreeSurfer analysis is the gold standard for cortical thickness measurements, which employs the surface-based technique, and takes a long time to analyze [12]. FreeSurfer (http://surfer.nmr.mgh.harvard.edu/) with the recon-all process flow was used to build a 3D cortical surface model from the T1W images [13]. After an automated Talairach transformation, nonbrain tissue removal, hemisphere separation, and cerebellum and brain stem removal were performed. Then, the GM and WM surface borders were reconstructed [12]. Cortical thickness was accepted as the pial surface-WM distance [13]. After the automatic reconstruction, possible misclassification was visually checked. Using the Desikan–Killiany atlas, the mean cortical thickness values were averaged for 34 ROIs [14]. Then, the ROI results of both groups were statistically compared.

2.5. Statistical analysis

SPSS was used to perform the statistical analysis. Complementary statistical methods were used to evaluate the data (mean, standard deviation, median, frequency, percentage, minimum, and maximum). Quantitative variables without normal distribution were compared between 2 groups using the Mann–Whitney U test and Kruskal–Wallis test. Patient and healthy group comparisons of the nonnormal variables was performed using the Wilcoxon signed-rank test. Statistical significance was accepted as $p < 0.05$. In the VBM analysis, a 1-tailed significance threshold was set at voxel-level uncorrected $p < 0.001$ and cluster-level family-wise error (FWE)-corrected $p < 0.05$ [15].

3. Results

Herein, 20 ESES patients were initially considered. After taking into account the exclusion criteria, 12 ESES patients (33.3% female and 66.7% male) and 12 healthy controls (33.3% female and 66.7% male) were compared. The age and sex distribution was not significantly different between the groups. Whole exome sequencing (WES) was used to examine the ESES patients for genetic mutations. In 8 patients, one or more epilepsy genes, *GRIN2A, TET3, SCN1A, SCN8A, ADGRV1, DLG4*, and *SLC12A5*, were found, and 12 patients had no genetic mutations. Based on the exclusion criteria, 6 ESES patients with genetic mutations and 6 without were included.

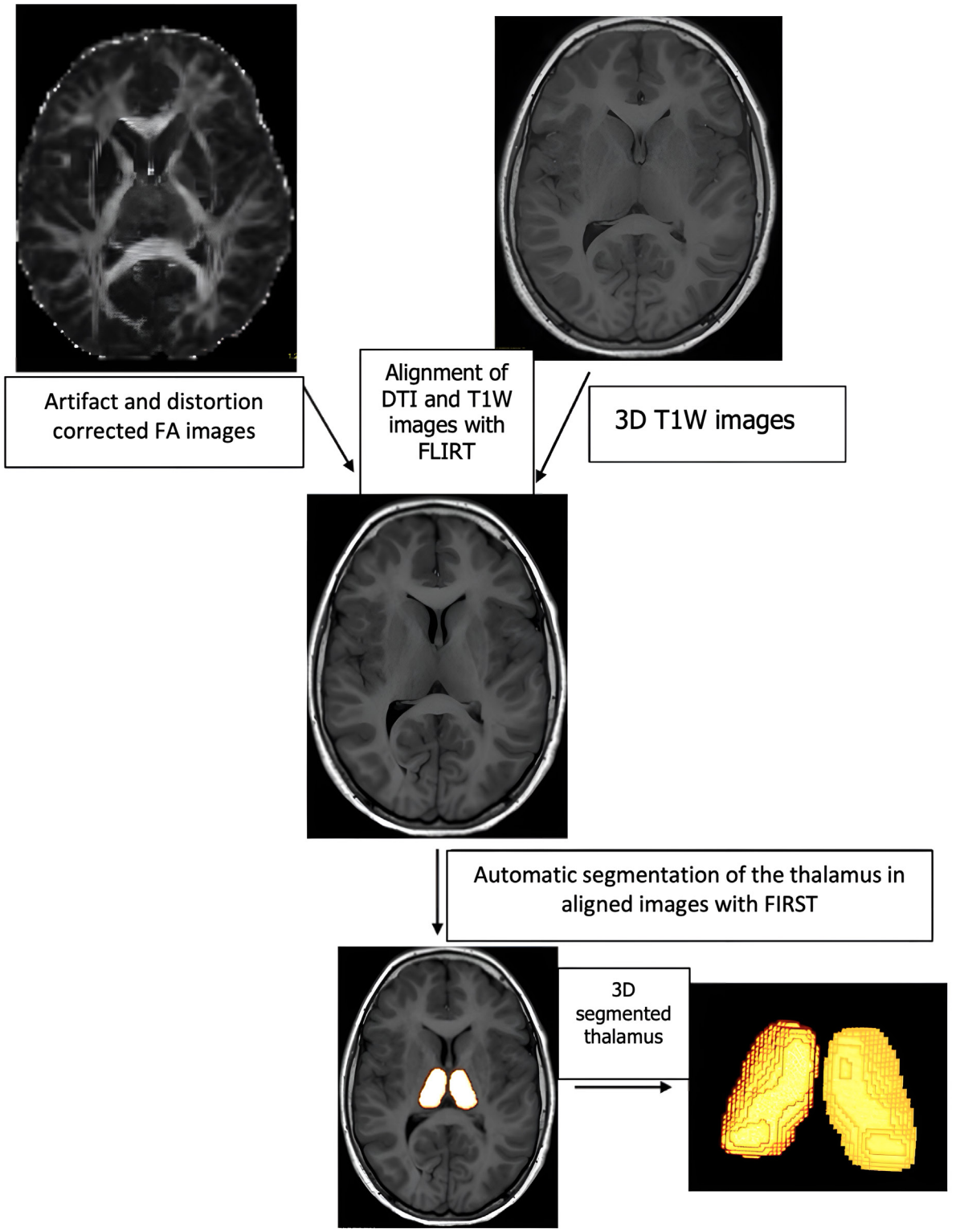


Figure 1. Schematic representation of the thalamus-specific analysis technique.

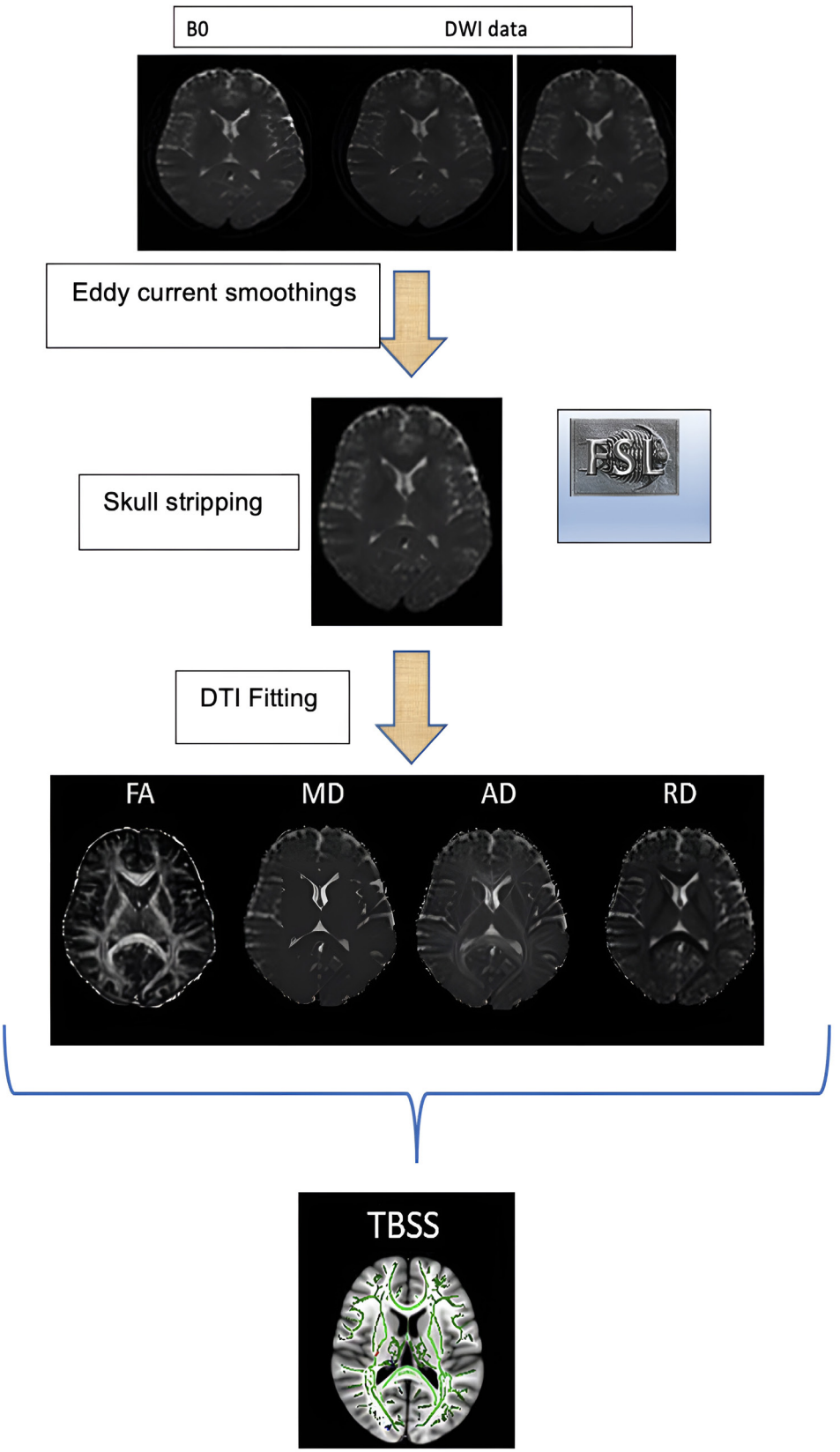


Figure 2. Schematic representation of the TBSS analysis.

Figure 3 shows the thalamus-specific volume-of-interest (TBSS-VOI) analysis findings from the DTI and TBSS analysis. The ESES patients had significantly higher MD in their thalamus than the controls ($p = 0.042$). Differences between the groups in the FA, AD, and RD were not significant ($p > 0.05$). The WM TBSS analysis showed no significant differences in the FA, MD, AD, and RD between the control, mutation-positive, and mutation-negative groups ($p > 0.05$) (Table 1). The Kruskal–Wallis test showed that the mutation-positive ESES patients had decreased AD in the superior longitudinal fasciculus (SLF) (Figure 4).

VBM analysis, which analyzes the chance of a voxel having GM-WM-BOS, showed no statistically significant difference between the mutation-negative and control groups. Mutation-positive patients showed a decreased GM volume in the left entorhinal area, bilateral putamen, bilateral cerebral WM, left accumbens, left caudate, and bilateral cerebellum exterior (Table 2, Figure 5a). Figure 5b shows glass brain images of the same locations.

Specific curvature differences were analyzed in the ESES patients with genetic abnormalities using a local gyrification index analysis since it may indicate developmental disorders. No significant difference was found across the groups.

Subcortical shape analysis was used to extract and statistically compare 15 right and left subcortical structures and the 3D thalamus shape. Shape changes precede the volume changes, which is what makes this method sensitive. The bilateral thalamus, accumbens, hippocampus, putamen, caudate nucleus, and amygdala of the patients were not significantly different.

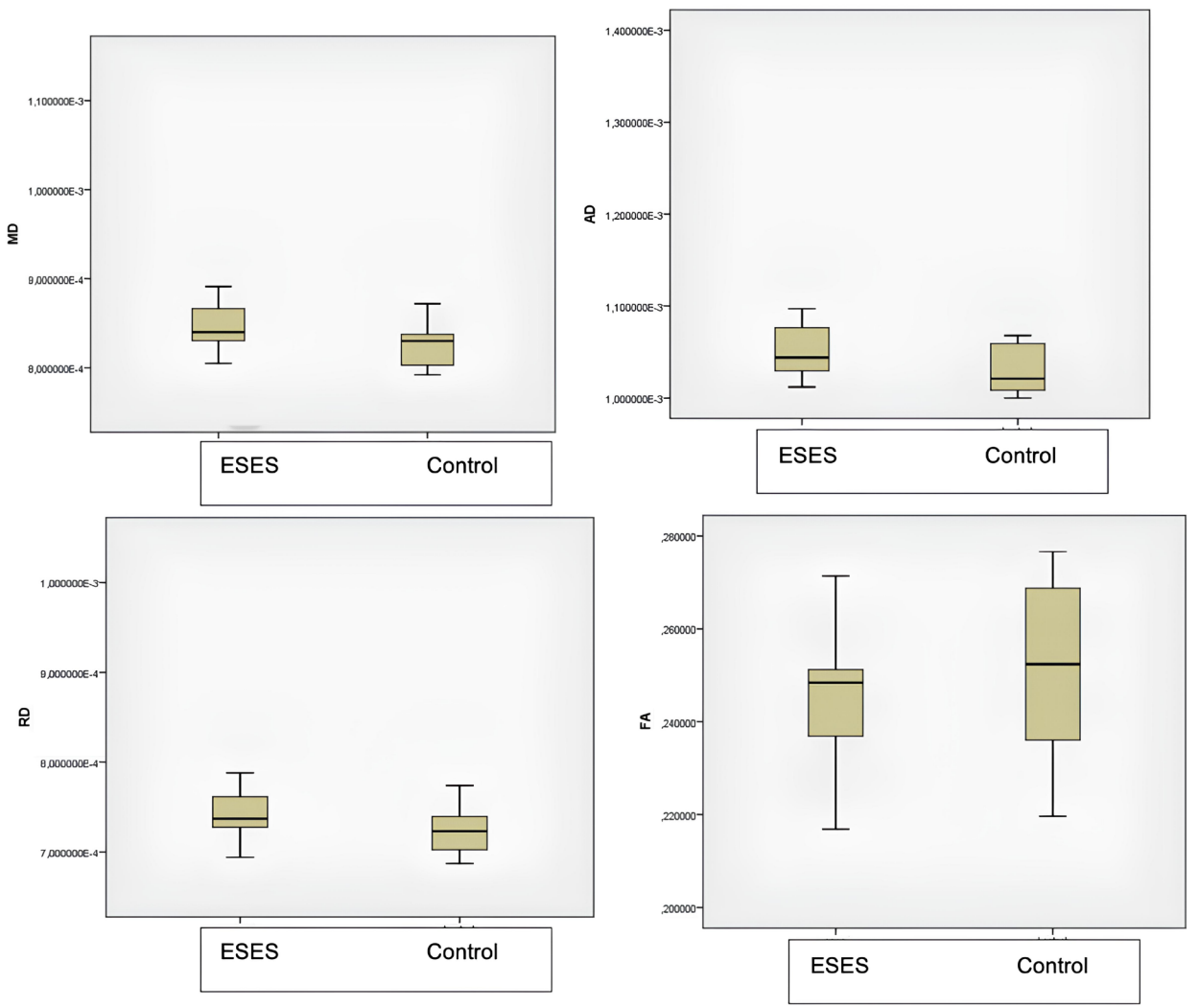


Figure 3. ROI analysis of the AD, FA, MD, RD values in the ESES and control groups.

Table 1. Thalamus-specific tract-based spatial statistics (TBSS)-volume of interest (VOI) analysis results of the ESES patients compared to the healthy control group.

Group		Mean	SD[b]	p-value[c]
FA[a]	ESES	0.24318375	0.005431528	0.242
	Control	0.25105600	0.006151309	
MD[a]	ESES	0.00086583	0.000024712	0.042
	Control	0.00082491	0.000007601	
AD[a]	ESES	0.00107000	0.000081912	0.060
	Control	0.00103009	0.000027271	
RD[a]	ESES	0.00076367	0.000025483	0.124
	Control	0.00072245	0.000008137	

a: FA: fractional anisotropy, MD: mean diffusion, AD: axial diffusion, RD: radial diffusion, b: SD: standard deviation, c: Mann–Whitney U test.

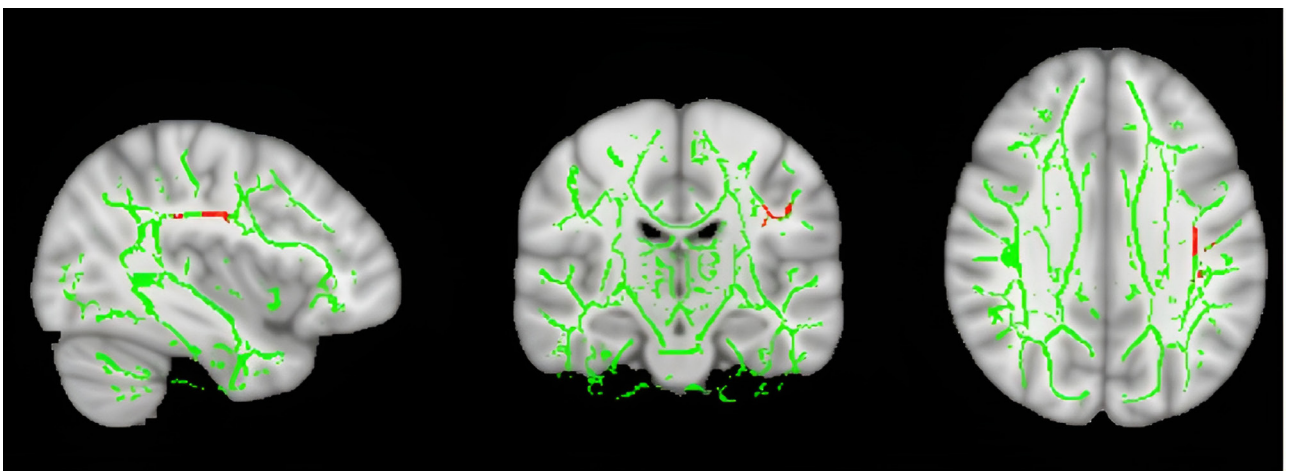


Figure 4. Comparison of the ESES groups with and without genetic mutations, areas showing increased AD in patients with mutations.

Table 2. Decrease in GM volume observed in the genetic mutation-positive ESES patients compered to mutation-negative patients.

Cluster index	Labels[a]	Cluster size	x, y, z (mm)[b]	p-value[c]
1	Right cerebellum exterior 92%	78	8, –82, –32	6.08
2	Right cerebellum exterior 98%	245	33, –72, –24	5.72
	Right occipital fusiform gyrus 2%			
3	Left cerebellum exterior 100%	78	–33, –72, –28	5.47
4	Right cerebellum exterior 100%	68	24, –68, –21	5.16
5	Left entorhinal area 96%	80	–22, 0, –28	5.14
	Left fusiform gyrus 4%			
6	Left cerebellum exterior 94%	35	–27, –72, –24	5.09
	Left occipital fusiform gyrus 6%			
7	Left cerebellum exterior 100%	46	–39, –81, –28	4.60
8	Left putamen 100%	92	–24, 4, 10	4.58

a: Labels according to a Desikan Killiany atlas in CAT12. The percentiles given next to the regions show how much of the vertices in that cluster belong to that region, b: According to the MNI coordinate system, c: VBM at a threshold of voxel-level uncorrected $p < 0.001$ and cluster-level FWE corrected $p < 0.05$ (Poline et al., 1997) for omissions and superordinate errors.

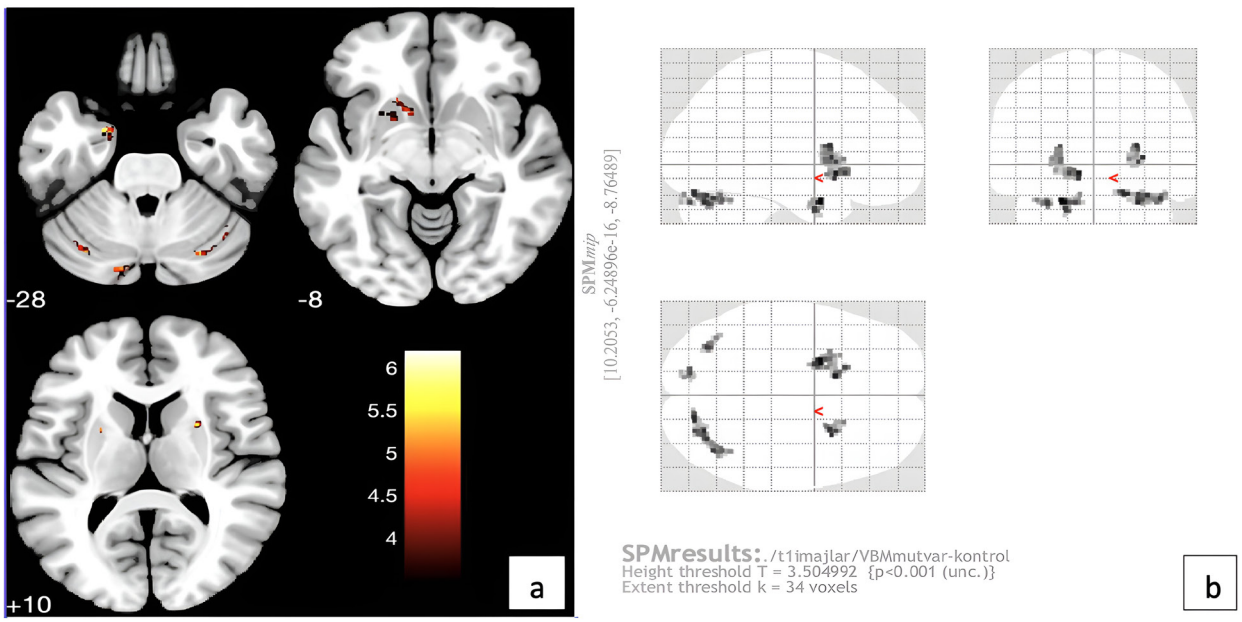


Figure 5. VBM analysis: (a) Locations of decreased GM volume in the mutation-positive ESES: Left entorhinal area, left putamen, left cerebral WM, left accumbens area, left caudate, right cerebellum exterior, right putamen, right cerebral WM, left cerebellum exterior, left cerebellum exterior, and (b) the appearance of the same areas in the glass brain image.

Figure 6 shows the FreeSurfer volume and cortical thickness analyses. The superior and middle temporal cortical thickness in the ESES patients were determined to increase using FreeSurfer.

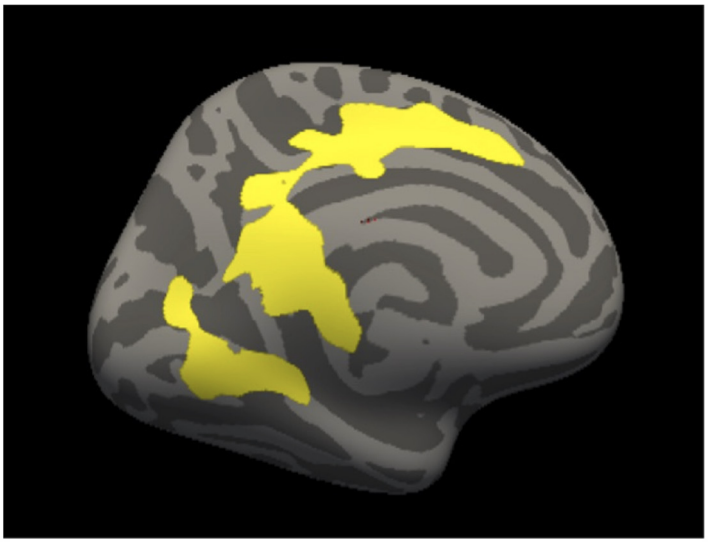
4. Discussion

This microstructural brain study of ESES patients with and without genetic mutations utilizing DTI-TBSS analysis, VBM, a local gyrification index, subcortical shape analysis, and FreeSurfer volume-cortical thickness analysis differs from the literature. Multiple analytic approaches including thalamus-specific analysis assessed GM and WM structural changes in ESES patients.

In our TBSS-VOI analysis, ESES patients' thalamus MD increased. The thalamus and thalamocortical circuit have been studied for ESES's etiopathogenesis. The literature attributes thalamic physiological oscillations to the cyclic interaction between glutaminergic excitatory thalamocortical neurons in the dorsal thalamic nuclei and inhibitory GABAergic neurons in the reticular nuclei [16,17]. ESES patients exhibit thalamic involvement during interictal epileptic discharges [18], and early thalamic lesions may damage the corticothalamic circuit, causing ESES [19]. Parenchymal damage is usually present [20]. Thalamic volume and metabolic changes can be seen in ESES but are complex [1,21–23]. These studies cannot explain etiopathogenesis without structural thalamic lesions.

In our study, MD, which measures total diffusion, increased in ESES patients without thalamic lesions, indicating thalamic integrity loss and microstructural involvement. In the Cuprizone mouse model, AD (water molecule diffusion parallel to WM tracts) decreases, indicating axonal degeneration and early demyelination [24]. Genetically mutant ESES patients have decreased SLF AD. SLF is a WM structure with long, bidirectional projections between the prefrontal, temporal, occipital, and parietal cortices. The Human Connectome Project DTI template clarifies its anatomical characteristics but not its neurobehavioral functions. Its anatomical location suggests it contributes to several cognitive domains, including visuospatial non-verbal cognition and verbal memory. SLF DTI showed significant correlations between the left SLF, perceptual organization, and working memory [25]. In a pediatric study that evaluated the SLF's microstructural integrity, neuropsychiatric functions, and cognitive domain, FA and AD levels were positively correlated with executive functions [26]. One pathophysiologic reason for cognitive decline, memory impairment, and attention deficit in our ESES patients may be decreased AD in the left SLF.

In genetically mutated ESES patients, VBM showed reduce GM volumes in the corpus striatum, accumbens, entorhinal, and cerebellar outer part. This study showed that seizures develop with spike-wave (SWD) discharges



Size (mm^2)	MNIX	MNIY	MNIZ	
2933.50	66.2	-31.4	6.0	Superior temporal
1560.15	63.7	-30.6	-14.6	Middle temporal

Figure 6. FreeSurfer volume and cortical thickness analysis results: areas with increased cortical thickness in the ESES group; superior temporal and middle temporal.

initiated by decreased cortical excitatory transmission to the striatum, decreased excitatory transmission from the neocortex to striatal fast-spiking interneurons, SWDs are suppressed when AMPA receptors in the striatum are potentiated, and disruption of cortico-striatal excitatory transmission in haplodeficient mice causes epilepsy [27]. Corticostriatal transmission may explain the corpus striatum GM volume reduction in our genetically mutated ESES patients. Large genetic-based studies on this field may help evaluate new disease treatment targets like DBS and develop treatments.

The mesolimbic pathway involving the nucleus accumbens (Nacc) stores memories and is a reward circuit [28]. Nacc abnormalities, Nacc neuron degeneration, and abnormal neuroactive substance distribution are linked to refractory epilepsy's pathophysiology. In refractory epilepsy, Nacc involvement has been linked to motivational-emotional processes, limbic-motor interfaces, and clinical findings. It may be a therapeutic target [29]. The role of Nacc in ESES ictogenesis and epileptogenesis has been supported by decreased ventral striatum accumbens GM volume in our study. Our findings may explain ESES neuropsychiatric symptoms. However, they cannot explain the genetic mutation link, hence complete genetic studies are needed.

The entorhinal area transmits most cortical information to the hippocampus [30]. VBM study showed decreased entorhinal area GM volume in our genetically mutated ESES patients. Similarly, morphometric studies of mesial temporal epilepsy patients' hippocampus-related regions indicate a volume decrease. ESES patients' cognitive decline may be caused by entorhinal GM volume loss, which affects memory and memory-related paradigms [31].

Neuromodulation is being targeted beyond the epileptogenic center in epilepsy treatment. The cerebellum may be a therapeutic target in this scenario, and cerebellar modulation may strongly reduce seizures [32]. Cerebellar functional, structural, volumetric, and perfusional changes have been linked to epilepsy [33-36]. In addition to motor functions, the cerebellum is engaged in higher-order cognitive processes such hippocampus contextual computations [37, 38]. The numerous feed-back loops formed by input from the cortex via the pontine nuclei and output via the thalamus make the lateral cerebellar hemispheres part of the cerebrocerebellum [39]. Seizure susceptibility has been linked to the cerebellum's role in brain state modulation, particularly sleep-wake cycle management [40–43]. Cerebellar GM loss preceded SUDEP in a recent research. The cerebellum has been connected to seizure networks aside from epilepsy [32]. Structural changes affect cognition and patient outcomes and must be studied. We found GM volume decrease in the cerebellum exterior in ESES patients, suggesting treatment targets.

Our study identified no causal association between ESES-emphasized CTC cycle damage and rearrangements and their consequences. Our limited DTI array,

population's lack of structural thalamic lesions, small sample size, and lack of longitudinal assessments may explain this. Longitudinal studies will be beneficial for tracking the progression of processes.

The local gyrification index and subcortical shape analyses did not differ for the thalamus, hippocampus, amygdala, caudate, and putamen. This may have been due to the fact that the cross-sectional model, sample size, sample characteristics, underlying genetic factors or heterogeneity, the fact that most patients had started drug treatment, the duration of the disease and seizures, and the variability of treatment duration were technically determined.

The superior and middle temporal cortical thickness increased in the FreeSurfer analysis. Cortical thickness changes have numerous causes. Contrary to the results herein, temporal cortical thickness decreases have been associated with epilepsy duration and seizure frequency in general [5,44,45]. In temporal lobe epilepsy, glial, neuronal, and synaptic rearrangements may cause neocortex neuronal structural abnormalities similar to those in the hippocampus [46,47]. Cortical thickness changes may indicate long-term functional reorganization [48,49]. In the current study, the temporal cortical thickness may have varied due to increased CTC cycle activation and reorganization in ESES, treatment start date, seizure type, duration of the ictal-postictal interval, and seizure frequency. Cortical changes affect seizure frequency, duration, severity, and physiology [50]. ESES cortical interactions and processes require large and varied investigations.

Antiepileptic drugs might prevent cognitive deterioration and promote neurodevelopment if sophisticated MRI technologies identified people at high risk of ESES or in the prodromal phase when seizures began [4]. To rule out seizure types that may cause focal thalamic volume reduction, interictal epileptiform discharges, and chronic exposure to antiepileptic drug treatment, its effects, and disease duration, a prospective study with a large group of patients is needed.

This study did have some limitations. The patients included those with and without genetic abnormalities, even though the majority had begun therapy. The small sample size, limited DTI array, and lack of literature on ESES cases with genetic alterations were other limitations. Further studies with untreated patients may help us to understand the pathogenesis of ESES.

In conclusion, increased MD without thalamic structural lesions in ESES patients suggested volume-independent microstructural damage. Cognitive decline may be linked to decreased AD in SLF in ESES patients with genetic abnormalities in TBSS studies. In the VBM analysis, GM volume decreases in the corpus striatum, accumbens area, entorhinal area, and cerebellum exterior in the ESES patients with genetic mutations in the current study may have been related to corticostriatal transmission, ictogenesis, epileptogenesis, neuropsychiatric symptoms, cognitive decline, and cerebellar involvement, and these locations may be therapeutic targets in comprehensive studies. In the FreeSurfer analysis, increased cortical thickness at the superior and middle temporal levels may be linked to thalamocortical circuit activation, patient restructuring or treatment, seizure types, duration of the ictal-postictal period, and seizure frequency. In ESES, studies that combine DTI, volumetric assessment, metabolic changes, and fMRI may help to explain the physiology and etiopathogenesis of the CTC cycle and develop new therapeutic targets.

Conflict of interest

The authors declare that they have no conflicts of interest.

Funding

There was no funding provided for this study.

Informed consent

This study did not contain any studies with human participants or animals performed by any of the authors. This study was approved by the local medical ethical committee (2022/514/219/1), and all data were processed anonymously, according to the privacy legislation.

References

1. Sánchez Fernández I, Loddenkemper T, Peters JM, Kothare SV. Electrical status epilepticus in sleep: clinical presentation and pathophysiology. Pediatric Neurology 2012; 47 (6): 390-410. https://doi.org/10.1016/j.pediatrneurol.2012.06.016

2. Wiwattanadittakul N, Depositario-Cabacar D, Zelleke TG. Electrical status epilepticus in sleep (ESES)- treatment pattern and EEG outcome in children with very high spike-wave index. Epilepsy and Behavior 2020; 105: 106965. https://doi.org/10.1016/j.yebeh.2020.106965

3. Arican P, Gencpinar P, Olgac Dundar N, Tekgul H. Electrical status epilepticus during slow-wave sleep (ESES): current perspectives. Journal of Pediatric Neurosciences 2021; 16 (2): 91-96. https://doi.org/10.4103/jpn.JPN_137_20

4. Kilic H, Yilmaz K, Asgarova P, Kizilkilic O, Hatay GH et al. Electrical status epilepticus in sleep: the role of thalamus in etiopathogenesis. Seizure 2021; 93: 44-50. https://doi.org/10.1016/j.seizure.2021.10.010

5. Bernhardt BC, Worsley KJ, Besson P, Concha L, Lerch JP et al. Mapping limbic network organization in temporal lobe epilepsy using morphometric correlations: insights on the relation between mesiotemporal connectivity and cortical atrophy. Neuroimage 2008; 42 (2): 515-524. https://doi.org/10.1016/j.Neuroimage.2008.04.261

6. Han P, Stiller-Stut FP, Fjaeldstad A, Hummel T. Greater hippocampal gray matter volume in subjective hyperosmia: a voxel-based morphometry study. Scientific Reports 2020; 10 (1): 18869. https://doi.org/10.1038/s41598-020-75898-6

7. Li M, Yan J, Wen H, Lin J, Liang L et al. Cortical thickness, gyrification and sulcal depth in trigeminal neuralgia. Scientific Reports 2021; 11 (1): 16322. https://doi.org/10.1038/s41598-021-95811-z

8. Saini J, Sinha S, Bagepally BS, Ramchandraiah CT, Thennarasu K et al. Subcortical structural abnormalities in juvenile myoclonic epilepsy (JME): MR volumetry and vertex based analysis. Seizure 2013; 22 (3): 230-235. https://doi.org/10.1016/j.seizure.2013.01.001

9. Dahnke R, Yotter RA, Gaser C. Cortical thickness and central surface estimation. Neuroimage 2013; 65: 336-348. https://doi.org/10.1016/j.neuroimage.2012.09.050

10. Luders E, Thompson PM, Narr KL, Toga AW, Jancke L et al. A curvature-based approach to estimate local gyrification on the cortical surface. Neuroimage 2006; 29 (4): 1224-1230. https://doi.org/10.1016/j.neuroimage.2005.08.049

11. Patenaude B, Smith SM, Kennedy DN, Jenkinson MA. Bayesian model of shape and appearance for subcortical brain segmentation. Neuroimage 2011; 56 (3): 907-922. https://doi.org/10.1016/j.neuroimage.2011.02.046

12. Seiger R, Ganger S, Kranz GS, Hahn A, Lanzenberger R. Cortical thickness estimations of FreeSurfer and the CAT12 Toolbox in patients with Alzheimer's disease and healthy controls. Journal of Neuroimaging 2018; 28 (5): 515-523. https://doi.org/10.1111/jon.12521

13. Fischl B, Dale AM. Measuring the thickness of the human cerebral cortex from magnetic resonance images. Proceedings of the National Academy of Sciences of the United States of America 2000; 97 (20): 11050-11055. https://doi.org/10.1073/pnas.200033797

14. Desikan RS, Ségonne F, Fischl B, Quinn BT, Dickerson BC et al. An automated labeling system for subdividing the human cerebral cortex on MRI scans into gyral based regions of interest. Neuroimage 2006; 31 (3): 968-980. https://doi.org/10.1016/j.neuroimage.2006.01.021

15. Poline JB, Worsley KJ, Evans AC, Friston KJ. Combining spatial extent and peak intensity to test for activations in functional imaging. Neuroimage 1997; 5 (2): 83-96. https://doi.org/10.1006/nimg.1996.0248

16. Beenhakker MP, Huguenard JR. Neurons that fire together also conspire together: is normal sleep circuitry hijacked to generate epilepsy? Neuron 2009; 62 (5): 612-632. https://doi.org/10.1016/j.neuron.2009.05.015

17. Steriade M, McCormick DA, Sejnowski TJ. Thalamocortical oscillations in the sleeping and aroused brain. Science 1993; 262 (5134): 679-685. https://doi.org/10.1126/science.8235588

18. Siniatchkin M, Groening K, Moehring J, Moeller F, Boor R et al. Neuronal networks in children with continuous spikes and waves during slow sleep. Brain 2010; 133 (9): 2798-2813. https://doi.org/10.1093/brain/awq183

19. Leal A, Calado E, Vieira JP, Mendonça C, Ferreira JC et al. Anatomical and physiological basis of continuous spike-wave of sleep syndrome after early thalamic lesions. Epilepsy and Behavior 2018; 78: 243-255. https://doi.org/10.1016/j.yebeh.2017.08.027

20. Gibbs SA, Nobili L, Halász P. Interictal epileptiform discharges in sleep and the role of the thalamus in encephalopathy related to status epilepticus during slow Sleep. Epileptic Disorders 2019; 21 (S1): 54-61. https://doi.org/10.1684/epd.2019.1058

21. Agarwal R, Kumar A, Tiwari VN, Chugani H. Thalamic abnormalities in children with continuous spike-wave during slow-wave sleep: an F-18-fluorodeoxyglucose positron emission tomography perspective. Epilepsia 2016; 57 (2): 263-271. https://doi.org/10.1111/epi.13278

22. Sánchez Fernández I, Peters JM, Akhondi-Asl A, Klehm J, Warfield SK et al. Reduced thalamic volume in patients with electrical status epilepticus in sleep. Epilepsy Research 2017; 130: 74-80. https://doi.org/10.1016/j.eplepsyres.2017.01.010

23. Öztürk Z, Karalok ZS, Güneş A. Reduced thalamic volume is strongly associated with electrical status epilepticus in sleep. Acta Neurologica Belgica 2021; 121 (1): 211-217. https://doi.org/10.1007/s13760-019-01202-7

24. Song SK, Yoshino J, Le TQ, Lin SJ, Sun SW et al. Demyelination increases radial diffusivity in corpus callosum of mouse brain. Neuroimage 2005; 26 (1): 132-140. https://doi.org/10.1016/j.neuroimage.2005.01.028

25. Koshiyama D, Fukunaga M, Okada N, Morita K, Nemoto K et al. Association between the superior longitudinal fasciculus and perceptual organization and working memory: a diffusion tensor imaging study. Neuroscience Letters 2020; 738: 135349. https://doi.org/10.1016/j.neulet.2020.135349

26. Urger SE, de Bellis MD, Hooper SR, Woolley DP, Chen SD et al. The superior longitudinal fasciculus in typically developing children and adolescents: diffusion tensor imaging and neuropsychological correlates. Journal of Child Neurology 2015; 30 (1): 9-20. https://doi.org/10.1177/0883073813520503

27. Miyamoto H, Tatsukawa T, Shimohata A, Yamagata T, Suzuki T et al. Impaired cortico-striatal excitatory transmission triggers epilepsy. Nature Communications 2019; 10 (1): 1917. https://doi.org/10.1038/s41467-019-09954-9

28. Volman SF, Lammel S, Margolis EB, Kim Y, Richard JM et al. New insights into the specificity and plasticity of reward and aversion encoding in the mesolimbic system. Journal of Neuroscience 2013; 33 (45): 17569-17576. https://doi.org/10.1523/JNEUROSCI.3250-13.2013

29. Wang J, Zhang Y, Zhang H, Wang K, Wang H et al. Nucleus accumbens shell: a potential target for drug-resistant epilepsy with neuropsychiatric disorders. Epilepsy Research 2020; 164: 106365. https://doi.org/10.1016/j.eplepsyres.2020.106365

30. Bonilha L, Rorden C, Castellano G, Pereira F, Rio PA et al. Voxel-based morphometry reveals gray matter network atrophy in refractory medial temporal lobe epilepsy. Archives of Neurology 2004; 61 (9), 1379–1384. https://doi.org/10.1001/archneur.61.9.1379

31. Garcia AD, Buffalo EA. Anatomy and function of the primate entorhinal cortex. Annual Review of Vision Science 2020; 6: 411-432. https://doi.org/10.1146/annurev-vision-030320-041115

32. Streng ML, Krook-Magnuson E. The cerebellum and epilepsy. Epilepsy and Behavior 2021; 121 (Pt B): 106909. https://doi.org/10.1016/j.yebeh.2020.106909

33. Buijink AWG, Caan MWA, Tijssen MAJ, Hoogduin JM, Maurits NM et al. Decreased cerebellar fiber density in cortical myoclonic tremor but not in essential tremor. Cerebellum 2013; 12 (2): 199-204. https://doi.org/10.1007/s12311-012-0414-2

34. Allen LA, Vos SB, Kumar R, Ogren JA, Harper RK et al. Cerebellar, limbic, and midbrain volume alterations in sudden unexpected death in epilepsy. Epilepsia 2019; 60 (4): 718-729. https://doi.org/10.1111/epi.14689

35. Wiest R, Estermann L, Scheidegger O, Rummel C, Jann K et al. Widespread grey matter changes and hemodynamic correlates to interictal epileptiform discharges in pharmacoresistant mesial temporal epilepsy. Journal of Neurology 2013; 260 (6): 1601-1610. https://doi.org/10.1007/s00415-013-6841-2

36. Bohnen NI, O'Brien TJ, Mullan BP, So EL. Cerebellar changes in partial seizures: clinical correlations of quantitative SPECT and MRI analysis. Epilepsia 1998; 39 (6): 640-650. https://doi.org/10.1111/j.1528-1157.1998.tb01433.x

37. Popa LS, Hewitt AL, Ebner TJ. The cerebellum for jocks and nerds alike. Frontiers in Systems Neuroscience 2014; 8: 113. https://doi.org/10.3389/fnsys.2014.00113

38. Sokolov AA, Miall RC, Ivry RB. The cerebellum: adaptive prediction for movement and cognition. Trends in Cognitive Sciences 2017; 21 (5): 313-332. https://doi.org/10.1016/j.tics.2017.02.005

39. Kandel ER, Schwartz JH, Jessell TM, Siegelbaum SA, Hudspeth AJ, Mack S (editors). Principles of Neural Science. 5th ed. McGraw Hill; 2014.

40. Canto CB, Onuki Y, Bruinsma B, van der Werf YD, de Zeeuw CI. The sleeping cerebellum. Trends in Neurosciences 2017; 40 (5): 309-23. https://doi.org/10.1016/j.tins.2017.03.001

41. Ewell LA, Liang L, Armstrong C, Soltész I, Leutgeb S et al. Brain state is a major factor in preseizure hippocampal network activity and influences success of seizure intervention. Journal of Neuroscience 2015; 35 (47): 15635-15648. https://doi.org/10.1523/JNEUROSCI.5112-14.2015

42. Khan S, Nobili L, Khatami R, Loddenkemper T, Cajochen C et al. Circadian rhythm and epilepsy. Lancet Neurology 2018; 17 (12): 1098-1108. https://doi.org/10.1016/S1474-4422(18)30335-1

43. Purnell BS, Thijs RD, Buchanan GF. Dead in the night: sleep-wake and time-of-day influences on sudden unexpected death in epilepsy. Frontiers in Neurology 2018; 9: 1079. https://doi.org/10.3389/fneur.2018.01079

44. Lin JJ, Salamon N, Lee AD, Dutton RA, Geaga JA et al. Reduced neocortical thickness and complexity mapped in mesial temporal lobe epilepsy with hippocampal sclerosis. Cerebral Cortex 2007; 17 (9): 2007-2018. https://doi.org/10.1093/cercor/bhl109

45. Bernhardt BC, Rozen DA, Worsley KJ, Evans AC, Bernasconi N et al. Thalamo-cortical network pathology in idiopathic generalized epilepsy: insights from MRI-based morphometric correlation analysis. Neuroimage 2009; 46 (2): 373-381. https://doi.org/10.1016/j.neuroimage.2009.01.055

46. Salin P, Tseng G, Hoffman S, Parada I, Prince DA. Axonal sprouting in layer V pyramidal neurons of chronically injured cerebral cortex. Journal of Neuroscience 1995; 15 (12): 8234-8245. https://doi.org/10.1523/JNEUROSCI.15-12-08234.1995

47. Colciaghi F, Finardi A, Nobili P, Locatelli D, Spigolon G et al. Progressive brain damage, synaptic reorganization and NMDA activation in a model of epileptogenic cortical dysplasia. PLoS One 2014; 9 (2): e89898. https://doi.org/10.1371/journal.pone.0089898

48. Elger CE, Helmstaedter C, Kurthen M. Chronic epilepsy and cognition. The Lancet Neurology 2004; 3 (11): 663-672. https://doi.org/10.1016/S1474-4422(04)00906-8

49. McDonald CR, Hagler DJ, Jr Ahmadi ME, Tecoma E, Iragui V et al. Regional neocortical thinning in mesial temporal lobe epilepsy. Epilepsia 2008; 49 (5): 794-803. https://doi.org/10.1111/j.1528-1167.2008.01539.x

50. Ogren JA, Tripathi R, Macey PM, Kumar R, Stern JM et al. Regional cortical thickness changes accompanying generalized tonic-clonic seizures. NeuroImage: Clinical 2018; 20: 205-215. https://doi.org/10.1016/j.nicl.2018.07.015